Morphology and mechanical properties of hydroxypropyl cellulose cast films crosslinked in solution

Naoko Yanagida and Masaru Matsuo*
Department of Clothing Science, Faculty of Home Economics, Nara Women's University, Nara 630, Japan
(Received 3 January 1990; revised 21 December 1990; accepted 29 January 1991)

Glyoxal was used to crosslink hydroxypropyl cellulose (HPC) chains. The crosslinking was performed by introducing glyoxal into a water or ethanol solution of HPC at room temperature and allowing the solvent to evaporate under ambient conditions. The mechanical properties of the resultant films were estimated in relation to morphological properties, which were dependent upon the amount of glyoxal in solution. It turned out that a suitable amount of glyoxal causes a significant effect on crosslinking, while an excess amount of glyoxal causes drastic decreases in Young's modulus and tensile strength due to main-chain scission. The crosslinking of HPC molecules in solution could be estimated by dynamic light scattering. The diffusion coefficient and the Stokes radius were very sensitive to the degree of crosslinking. The former became lower and the latter became bigger on increasing the glyoxal content in solution. In contrast, an excess amount of glyoxal invoked the inverse relationship because of main-chain scission. These results indicate that the crosslinking effect in solution is sensitive to the morphology and mechanical properties of the resultant films.

(Keywords: glyoxal; crosslinking; hydroxypropyl cellulose; main-chain scission; dynamic light scattering)

INTRODUCTION

Cellulose plays an important role in the textile industry and in other industries, notably the paper industry and, as cellulose derivatives, in the paint industry. This is due to its characteristic properties of thermal stability, rigidity and water absorption. Hydroxyproyl cellulose (HPC) is a water-soluble cellulose derivative[1,2]. In this paper, the crosslinking of HPC molecules using glyoxal in solution was tried in order to develop materials with high water absorption. After crosslinking, the solvent was evaporated under ambient conditions. The morphology and mechanical properties of the resultant films were studied by wide-angle X-ray diffraction (WAXD), small-angle light scattering (SALS), optical microscopy and dynamic tensile modulus measurements. Furthermore, the diffusion coefficient and the Stokes radius of molecules in solution were estimated by dynamic light scattering. The estimation was done using histogram and cumulative methods. These values were discussed in relation to the effect of crosslinking of HPC chains in solution.

EXPERIMENTAL

The sample used in this experiment was HPC powder with a weight-average molecular weight $\bar{M}_w = 119.5 \times 10^4$ and a number-average molecular weight $\bar{M}_n = 26.8 \times 10^4$. These values, estimated by using gel permeation, were proposed by Dr Sudo of Yamagata University. The substitution of HPC is also expressed by Dr Sudo in terms of the molar substitution (MS), and the value was 4.25. The solvents were water and ethanol. A water (or ethanol) solution (300 ml) containing 5% (w/w) HPC was prepared by stirring for 5 h at room temperature. Then, glyoxal was introduced into the solution. The glyoxal contents chosen were 40, 6.25, 1.20, 0.67 and 0.22% (w/w). Films prepared with a glyoxal content $>40\%$ were torn by hand easily and no discussion is given for these specimens. The solution was stirred again for 5 h and subsequently hydrochloric acid (HCl) was introduced to perform crosslinking until the pH value of the solution had reached 0.8. Then, the solvent was allowed to evaporate under ambient conditions. The resultant films were immersed in an excess of ethanol for 1 h to remove residual traces of HCl.

The degree of swelling was defined as:

$$\frac{\text{weight of specimen in dry state}}{\text{weight of specimen containing water}} \times 100\ (\%)$$

Optical micrographs were obtained with a Nikon optical polarizer (XTP-11) and SALS patterns were obtained with a 3 mW He–Ne gas laser as the light source. X-ray measurements were carried out with a 12 kW rotating-anode X-ray generator (Rigaku RAD-rA). The WAXD and SAXS patterns were obtained with a flat camera using Cu K_α radiation at 200 mA and 40 kV. The complex dynamic tensile modulus functions were measured at a frequency of 10 Hz over the temperature range from $-70°C$ to the temperature corresponding to the breaking point of the specimen using a viscoelastic spectrometer (VES-F) obtained from Iwamoto Machine Co. Ltd. The details of the methods of measurement were described elsewhere[3–6].

*To whom correspondence should be addressed

0032-3861/92/050996-10

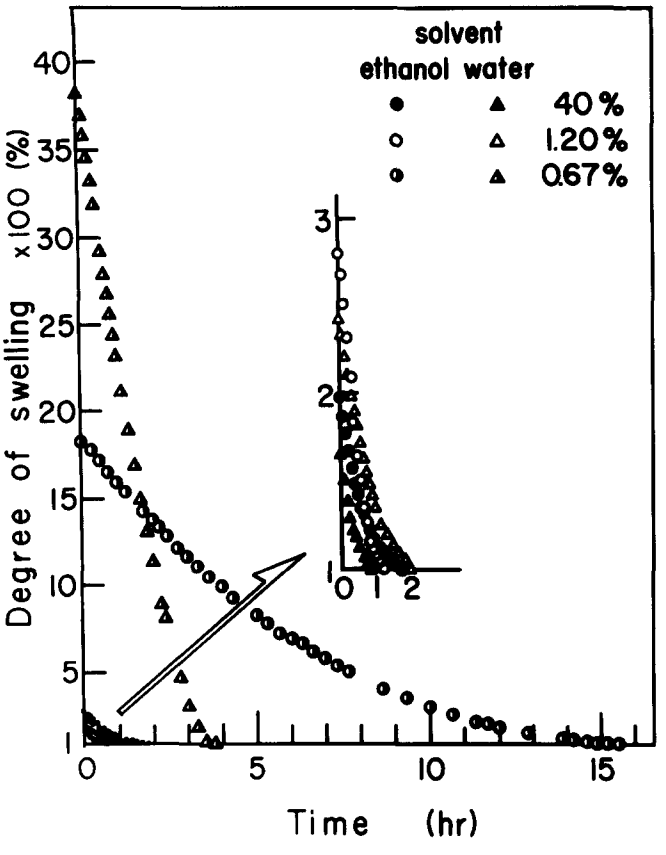

Figure 1 Time dependence of the degree of swelling of HPC films

The diffusion coefficient and the Stokes radius of HPC molecules in solution were analysed by histogram and cumulative methods on the basis of a correlation function measured by dynamic light scattering apparatus (DLS-700 obtained from Otsuka Electronics Co. Ltd) with a time interval digitizer[7–13].

RESULTS AND DISCUSSION

Figure 1 shows the time dependence of the degree of swelling of HPC films crosslinked with the indicated amounts (weight per cent) of glyoxal in water or ethanol solutions. The dried films were immersed in water for a week. The change in weight of the swollen film during evaporation of solvent at 50°C was measured by a special balance (EB-280MOC obtained from Shimazu Co. Ltd). The degree of swelling increased with decrease in glyoxal content, and this tendency is more pronounced in the case of the water cast film. The evaporation rate of water from the ethanol cast film is much slower than that from the water cast film, and water within the ethanol cast film crosslinked with 0.22% glyoxal was maintained for about 5 h. It is evident that the water absorption ability of the two kinds of films becomes much poorer at a glyoxal content $\geqslant 1.2\%$. This indicates the drastic increase in crosslink density with increasing content of glyoxal.

Figure 2 shows WAXD patterns (end view) from films crosslinked with the indicated glyoxal contents in water and ethanol solutions. The unit cell of the HPC crystal is tetragonal and the (1 0 0) and (0 1 0) reflections are equivalent[1]. All the patterns exhibit planar orientation of the (1 0 0) (or (0 1 0)) plane parallel to the film surface, and the amorphous chain segments are also oriented parallel to the film surface. This indicates that the molecular orientation of the resultant films is hardly affected by the degree of crosslinking.

Figure 3 shows WAXD intensity distributions of the crosslinked specimens cast from water or ethanol solution with various glyoxal contents. The peak height of the (1 0 0) plane at $2\theta = 7.8°$ becomes lower with increasing content of glyoxal, while that of the amorphous phase at $2\theta = 20.3°$ is hardly affected by the glyoxal content. This means that, although the content of the amorphous phase increases with increasing degree of crosslinking, X-ray diffraction is not sensitive enough to detect this behaviour.

Figure 4 shows the SALS patterns under the Hv polarization condition on the left and the corresponding optical micrographs (cross polarizers) on the right for the water cast specimens, while *Figure 5* shows the SALS pattern and the corresponding optical micrographs for the ethanol cast specimens. The SALS patterns are of the + type, indicating the characteristic scattering from rod-like textures[14–16], the optical axis being oriented at 45° with respect to the rod axis. The pattern becomes

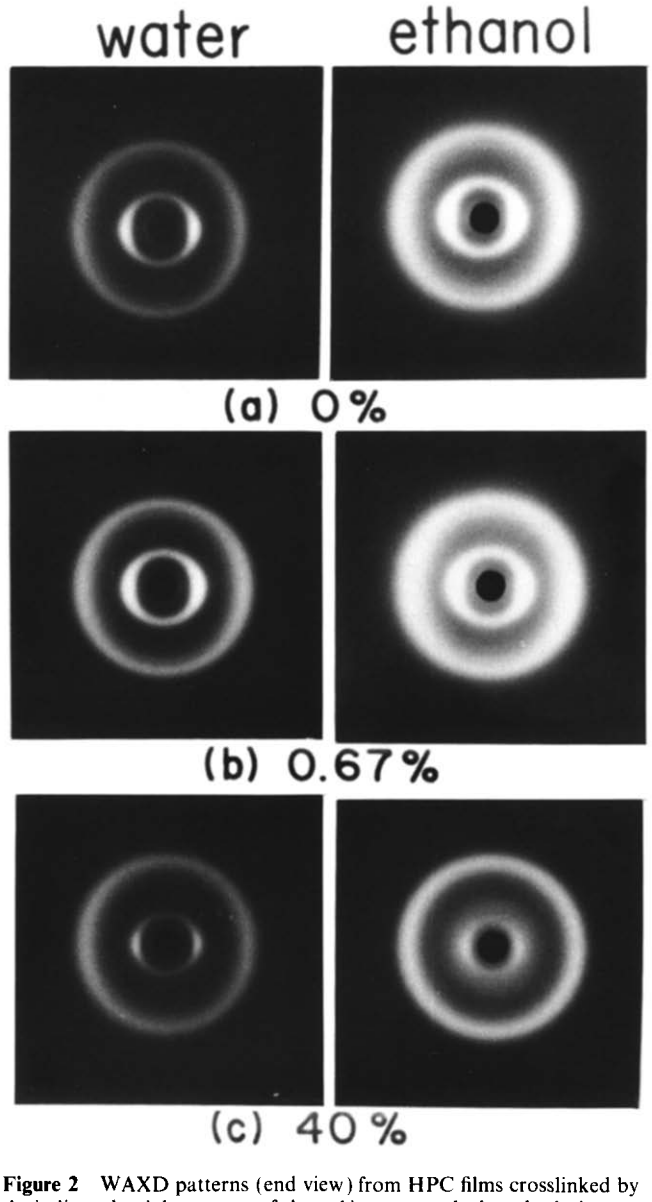

Figure 2 WAXD patterns (end view) from HPC films crosslinked by the indicated weight per cent of glyoxal in water and ethanol solutions

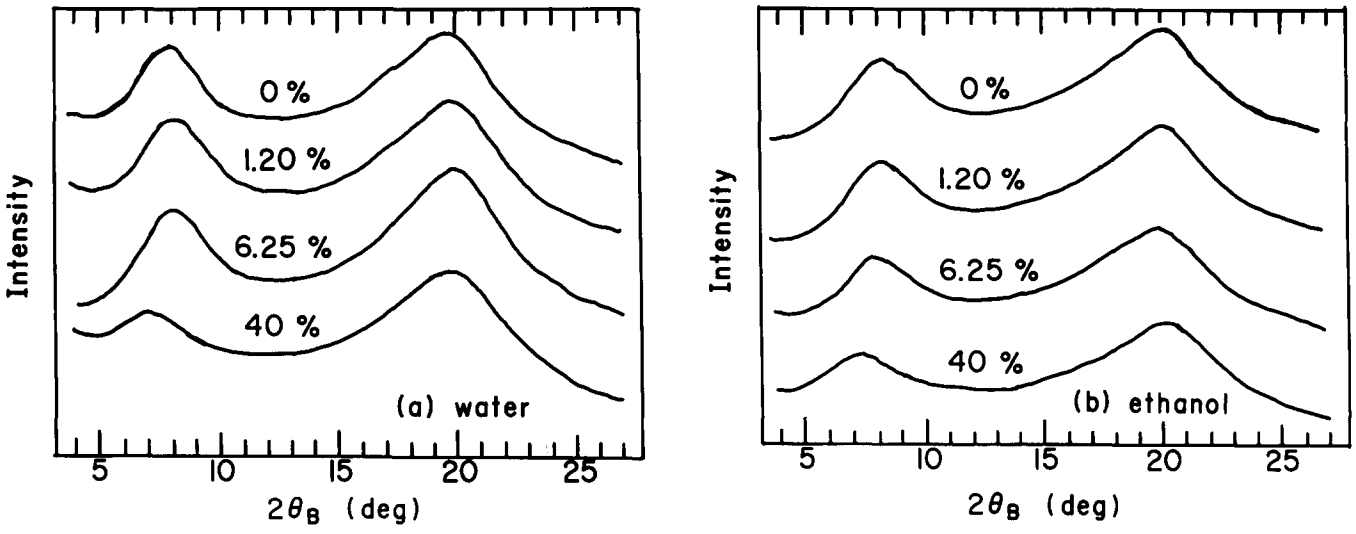

Figure 3 WAXD intensity distributions from specimens prepared from (a) water and (b) ethanol solutions with various contents of glyoxal

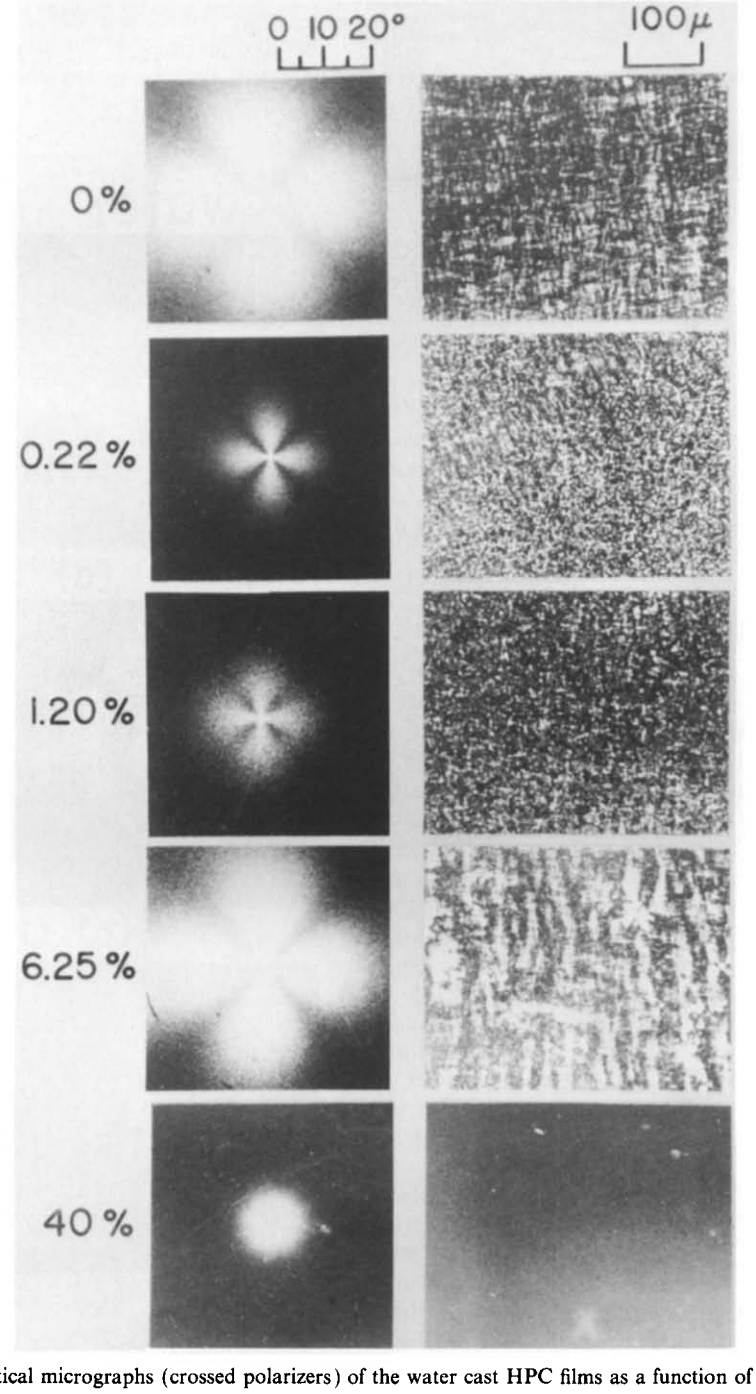

Figure 4 SALS patterns and optical micrographs (crossed polarizers) of the water cast HPC films as a function of glyoxal content

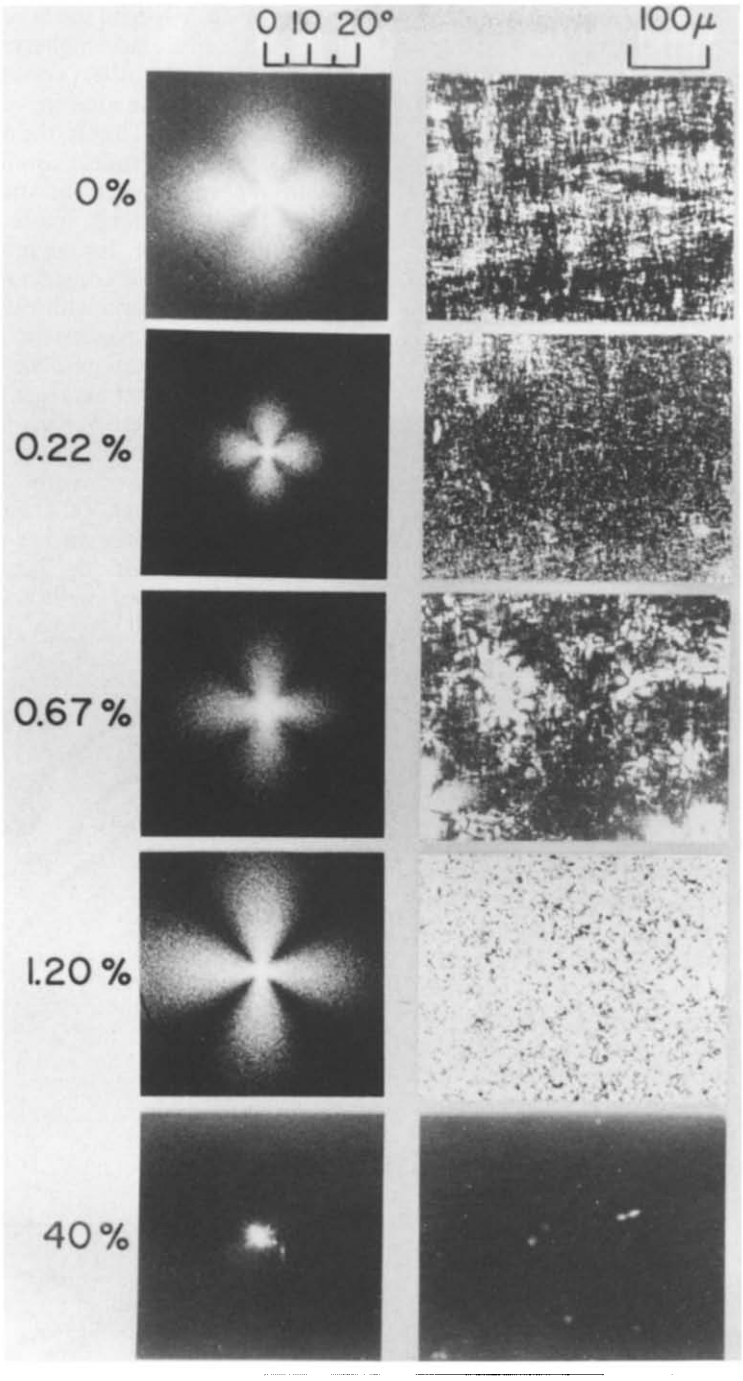

Figure 5 SALS patterns and optical micrographs (crossed polarizers) of the ethanol cast HPC films as a function of glyoxal content

smaller with increasing content of glyoxal up to 0.22% for the water and ethanol cast films. This indicates that the rod size becomes larger with increasing degree of crosslinking. However, when the content of glyoxal is beyond 1.2% for the water cast film and 0.67% for the ethanol cast film, the patterns become considerably larger. Beyond 40% for both specimens, however, the patterns become circular, indicating the typical scattering from a random array of crystallites that are small compared with the wavelength of the incident beam, and the corresponding optical micrographs show a dark field of vision. This indicates that no superstructure is observed in the optical microscope within the films crosslinked with 40% glyoxal. The resultant specimen is transparent, similar to amorphous polystyrene films. Here we must emphasize that the Hv pattern for 6.25% glyoxal in *Figure 4* does not reflect scattering from large fibrils as in the corresponding micrograph but scattering from small rods within the fibrils, since the size of the fibrils is too large to explain the scattering pattern at wider angle. Interestingly, an excess amount of glyoxal, such as 40%, hampers the formation of fibrils and rods, as discussed before. This is probably due to main-chain scission. To confirm this idea, the mechanical properties were measured for the uncrosslinked and crosslinked HPC films.

Figure 6 shows the nominal stress–strain relationship (a crosshead speed of 2 mm min^{-1}) of the crosslinked and uncrosslinked films at room temperature. The stress tends to level off beyond the yield point. The tensile

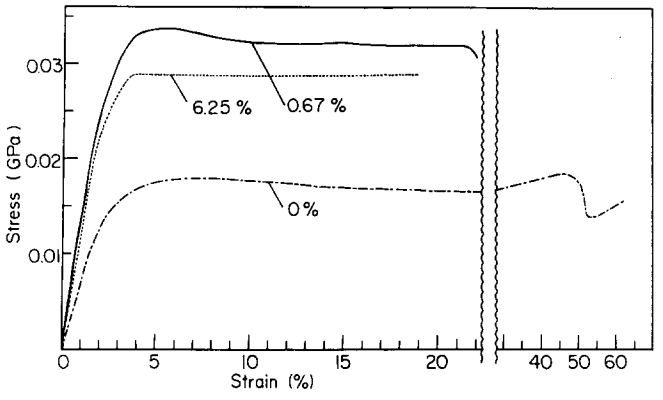

Figure 6 Nominal stress–strain relationship of the crosslinked and uncrosslinked HPC films at room temperature (crosshead speed of 2 mm min^{-1})

Table 1 The Young's modulus and tensile strength of water cast films of HPC crosslinked by the indicated contents of glyoxal

Glyoxal (wt%)	Young's modulus (GPa)	Tensile strength (MPa)
0	0.703	16
0.67	1.480	31
6.25	1.276	29

strength of the specimen crosslinked with 0.67% glyoxal in water solution is better than that of the specimen crosslinked with 6.25% glyoxal. This indicates that glyoxal causes main-chain scission in addition to crosslinking. This tendency becomes more pronounced as the glyoxal content increases beyond the most suitable amount for crosslinking. In fact, measurements of specimens crosslinked by glyoxal contents of 40% could not be carried out because of breaking at strains smaller than 1% and the films crosslinked by glyoxal content beyond 40% could be torn by hand. Thus, only the storage and loss moduli were measured at small strains less than 0.2% for the films crosslinked by glyoxal content of 40%.

It should be noted that, in determining the stress corresponding to each elongation, the values of the tensile force were divided by the cross-sectional area of the original specimens. If the tensile force is divided by the cross-sectional area of the specimen at each elongation, the true stress, rather than the nominal stress, is obtained. The increase in true stress with strain is, of course, more marked.

The Young's moduli and the tensile strengths of the specimens are summarized in *Table 1*. It is evident that, unfortunately, an excess amount of glyoxal causes main-chain scission, thus reducing the tensile strength and the Young's modulus of the resultant film.

In order to check the heat-resistance effect as a function of glyoxal content, the temperature dependence of the complex dynamic tensile modulus was observed. *Figures 7* and *8* show the results for uncrosslinked and crosslinked specimens cast from water and ethanol solutions, respectively. As can be seen in these figures, a suitable amount of glyoxal plays an important role in crosslinking of HPC chains. However, specimens prepared from water and ethanol solutions containing 40% glyoxal were broken at around 140 and 80°C, indicating considerable main-chain scission. It may be noted that the storage moduli of both specimens at temperatures less than 140 and 80°C are the highest among the specimens crosslinked with other contents of glyoxal. This is probably due to the absence of superstructure as shown in *Figures 4* and *5*. That is, the existence of superstructure is well known to invoke a complicated stress distribution within the specimen, like stress concentration at the boundary of the superstructure. Thus, it may be expected that in this case the storage modulus of the specimens is not so sensitive to the considerable amount of main-chain scission in comparison with the stress concentration due to the existence of superstructure, while chain slippage becomes most pronounced because of the active mobility of chains, as the temperature increases. However, this still remains an unresolved problem. The suitable glyoxal content depends on the kind of solution. For example, specimens crosslinked with 6.25% glyoxal in water solution were kept at 300°C, in spite of lower values of the Young's modulus and tensile strength as listed in *Table 1*. In contrast, the heat-resistance effect of the specimen crosslinked with 6.25% glyoxal in ethanol

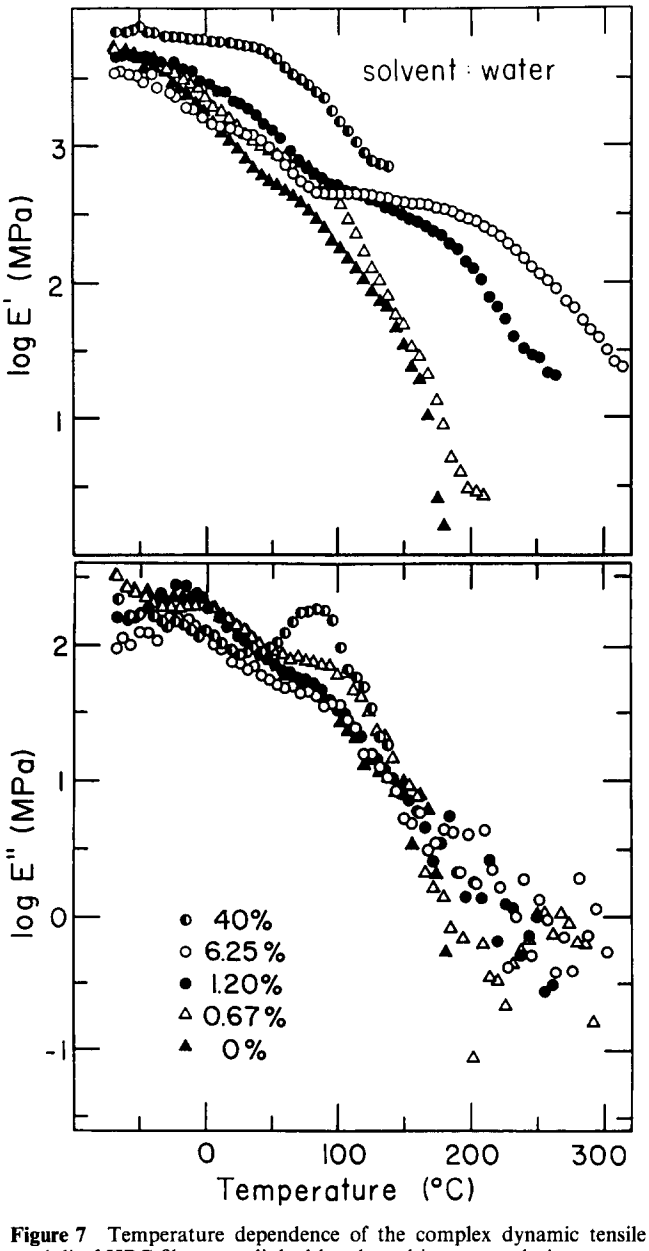

Figure 7 Temperature dependence of the complex dynamic tensile moduli of HPC films crosslinked by glyoxal in water solution

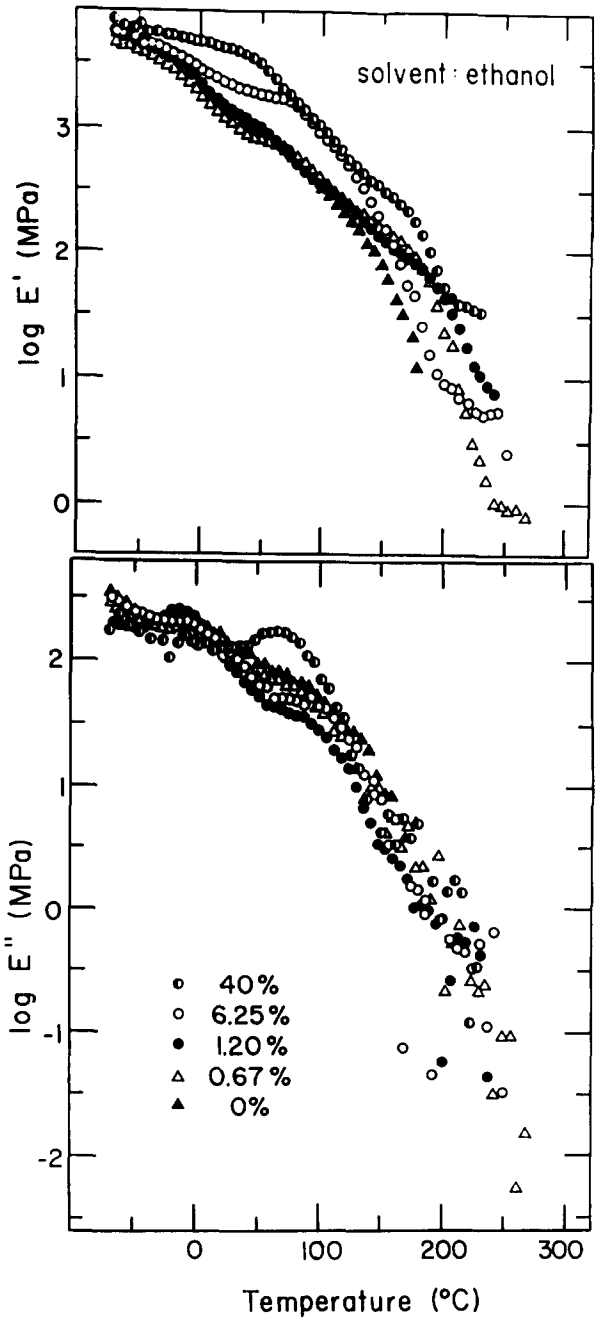

Figure 8 Temperature dependence of the complex dynamic tensile moduli of HPC films crosslinked by glyoxal in ethanol solution

solution is poorer than that of the specimen crosslinked with 0.67% glyoxal in water. Namely, the heat-resistance effect for the water cast films is sensitive to the amount of glyoxal, while this effect for the ethanol cast films is not so sensitive, and even the specimen crosslinked by 0.67% glyoxal, showing the best heat resistance, cannot be maintained beyond 270°C. This indicates that the chemical reaction causing crosslinking in ethanol solution is less pronounced than that in water. Judging from the results in *Figures 4–8*, it is evident that an excess of glyoxal hampers the formation of superstructure and causes the decrease of heat-resistance effect due to main-chain scission.

In order to facilitate understanding of the above concept, it is of interest to estimate the degree of crosslinking in solution in terms of the diffusion coefficient and the Stokes radius. Dynamic light scattering studies have been carried out for a narrow-distribution polystyrene, and the efficiency of the histogram method has been tested. As one application of dynamic light scattering, the crosslinking effect in solution was estimated for a polydisperse solution of HPC. The evaluation was done by the histogram and cumulative methods for determining the distribution of delay rate from the observed correlation function.

As described by Chu *et al.*, Tsunashima *et al.* and others[7–13] the normalized autocorrelation function $A(\tau)$ measured by the homodyne method under the Vv polarization condition is related to the normalized first-order correlation of the scattered elastic field, $g^{(1)}(\tau)$, by:

$$A(\tau) = 1 + \beta|g^{(1)}(\tau)|^2 \quad (1)$$

where τ is the delay time and β is a parameter determined by the experimental condition of coherence. For a monodisperse system, the correlation function $g^{(1)}(\tau)$ can be expressed as:

$$|g^{(1)}(\tau)| = \int_0^\infty G(\Gamma)\exp(-\Gamma\tau)\,d\Gamma \quad (2)$$

where $G(\Gamma)$ is the delay rate distribution. In the histogram method, $G(\Gamma)$ can be approximated by an equally segmented histogram extending over a region in Γ space. In the histogram method, equation (2) can be approximated by a histogram of equally segmented steps $\Delta\Gamma$ in Γ space:

$$|g^{(1)}(\tau)| = \sum_{j=1}^{m} H(\Gamma_j)\int_{\Gamma_j-\Delta\Gamma/2}^{\Gamma_j+\Delta\Gamma/2}\exp(-\Gamma\tau)\,d\Gamma \quad (3)$$

with the normalization condition:

$$\sum_{j=1}^{m} H(\Gamma_j)\Delta\Gamma = 1 \quad (4)$$

where $H(\Gamma_j)$ is the height of the jth histogram step of width $\Delta\Gamma$ around Γ_j and m is the number of steps. Hence

$$\Delta\Gamma = (\Gamma_{max} - \Gamma_{min})/m \quad (5)$$

where Γ_{min} and Γ_{max} are the lower and upper limits of the region. Substituting equation (3) into equation (1) yields:

$$A^*(\tau) = 1 + \beta\left(\sum_{j=1}^{m}[-H(\Gamma_j)/\tau]\{\exp[-(\Gamma_j + \tfrac{1}{2}\Delta\Gamma)\tau] - \exp[-(\Gamma_j - \tfrac{1}{2}\Delta\Gamma)\tau]\}\right)^2 \quad (6)$$

where $A^*(\tau)$ represents the computed function. The value of $H(\Gamma_j)$ can be determined by using the non-linear least-squares fitting procedure to minimize the fitting error of the computed function $A^*(\tau)$ to the observed one $A(\tau)$ with respect to each $H(\Gamma_j)$ simultaneously:

$$\frac{\partial}{\partial H(\Gamma_j)}\sum_i\{[A(i\Delta\tau) - A^*(i\Delta\tau)]^2/\sigma_i^2\} = 0 \quad (j = 1, 2, \ldots, m) \quad (7)$$

where $\Delta\tau$ is the clock pulse interval, i $(= \tau/\Delta\tau)$ is the channel number and σ_i are the uncertainties in the data points $A(i\Delta\tau)$. In actual calculations, the channel number i is set to be 128 or 256 and σ_i is fixed to be unity. The information of $H(\Gamma_j)$ gives the distribution

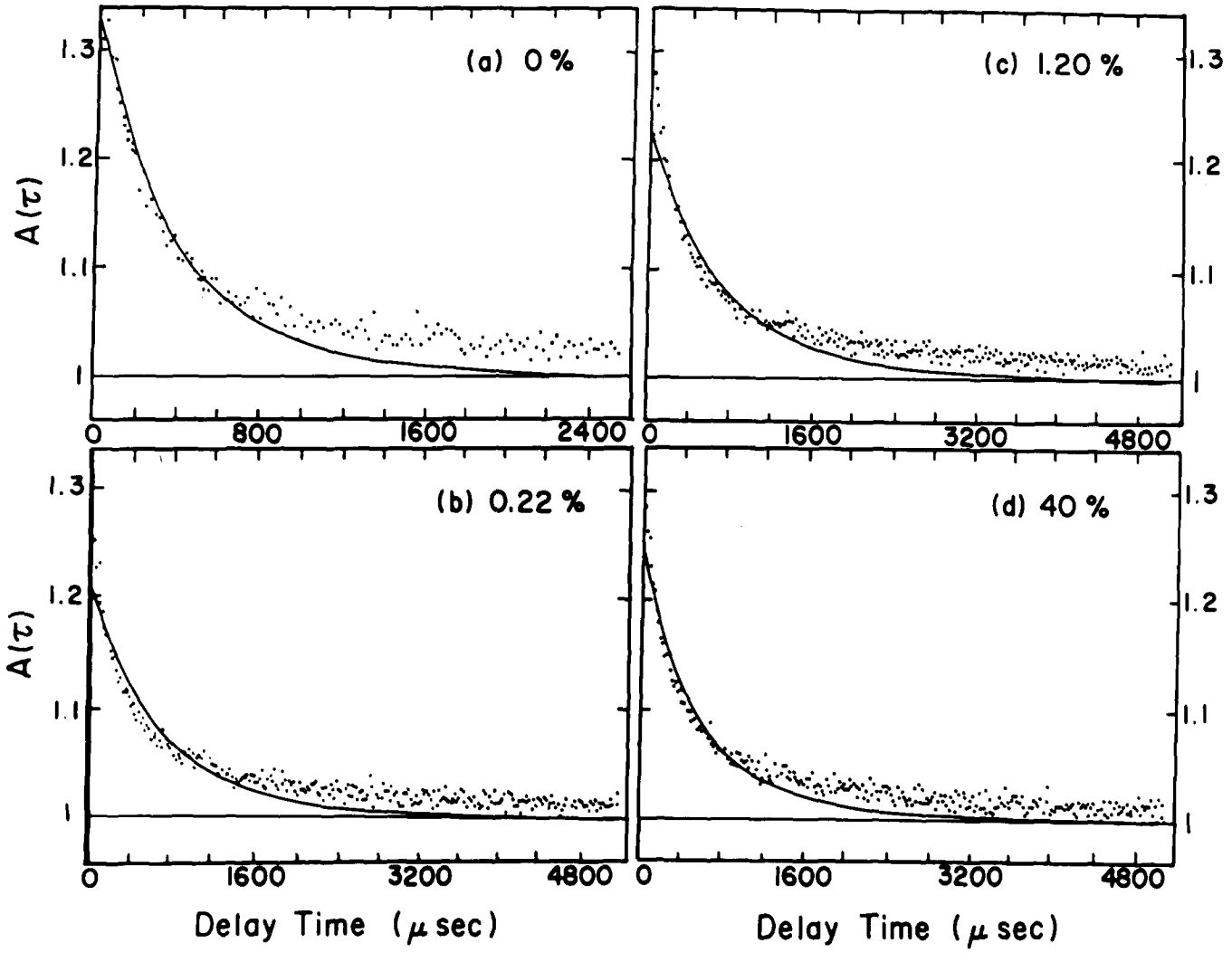

Figure 9 The autocorrelation functions $A(\tau)$ plotted against delay time τ and the function (full curves) recalculated from the histogram in *Figure 10* for the water solutions of HPC with various contents of glyoxal: (a) 0%, (b) 0.22%, (c) 1.20% and (d) 40%

of diffusion coefficient using the following relationship:

$$D_j = \Gamma_j/q^2 \tag{8}$$

where

$$q = (4\pi n/\lambda)\sin(\theta/2) \tag{9}$$

where n is the refractive index of solvent, λ is the wavelength of the incident beam in vaccum and θ is the scattering angle. In this experiment, θ is fixed to be 90°. The Stokes radius may be given by:

$$d_j = kT/6\pi\eta D_j \tag{10}$$

The distributions of weight fraction $w(d)$ and number fraction $n(d)$ can be calculated as follows:

$$w(d) = w(d_j)/[d_j^3 P(\theta = 90°)] \tag{11}$$

and

$$n(d) = w(d_j)/d_j^3 \tag{12}$$

where

$$P(\theta = 90°) = (3/x^3)^2(\sin x - x\cos x)^2 \tag{13}$$

and

$$x = (4\pi n/\lambda)\sqrt{2}/2 \tag{14}$$

Here, $g(d_j)$ corresponds to $H(\Gamma_j)$ in the case when Γ_j is replaced by d_j.

Figure 9 shows the autocorrelation functions $A(\tau)$ plotted against delay time τ for the HPC–water system with different contents of glyoxal measured by the homodyne method. The full curves are also autocorrelation functions recalculated from the histograms $H(\Gamma_j)$ shown in *Figure 10*. The calculation was carried out by assuming the unimodal system described before. This is based on a number of preliminary experimental results that the bimodal distribution gives a very complicated histogram but the autocorrelation function recalculated from the complicated histogram is similar to the autocorrelation function recalculated by assuming a unimodal distribution. The experimental results are in fairly good agreement with the calculated curve $A^*(\tau)$. Incidentally, for the present system, the assumption of the bimodal distribution is thought to be meaningless because of the complicated system associated with main-chain scission of HPC molecules with the broad molecular-weight distribution such as $\bar{M}_w/\bar{M}_n = 4.46$.

Figure 11 shows the frequency distributions of diffusion coefficient in the HPC–water system, corresponding to the frequency of $H(\Gamma_j)$ in *Figure 10*. The diffusion coefficients become lower with increasing glyoxal content up to 0.22%, indicating the decrease of chain mobility due to an increase in the degree of crosslink density. In contrast, as shown in *Figure 11d*, when the glyoxal content reached 40%, the diffusion coefficient decreased.

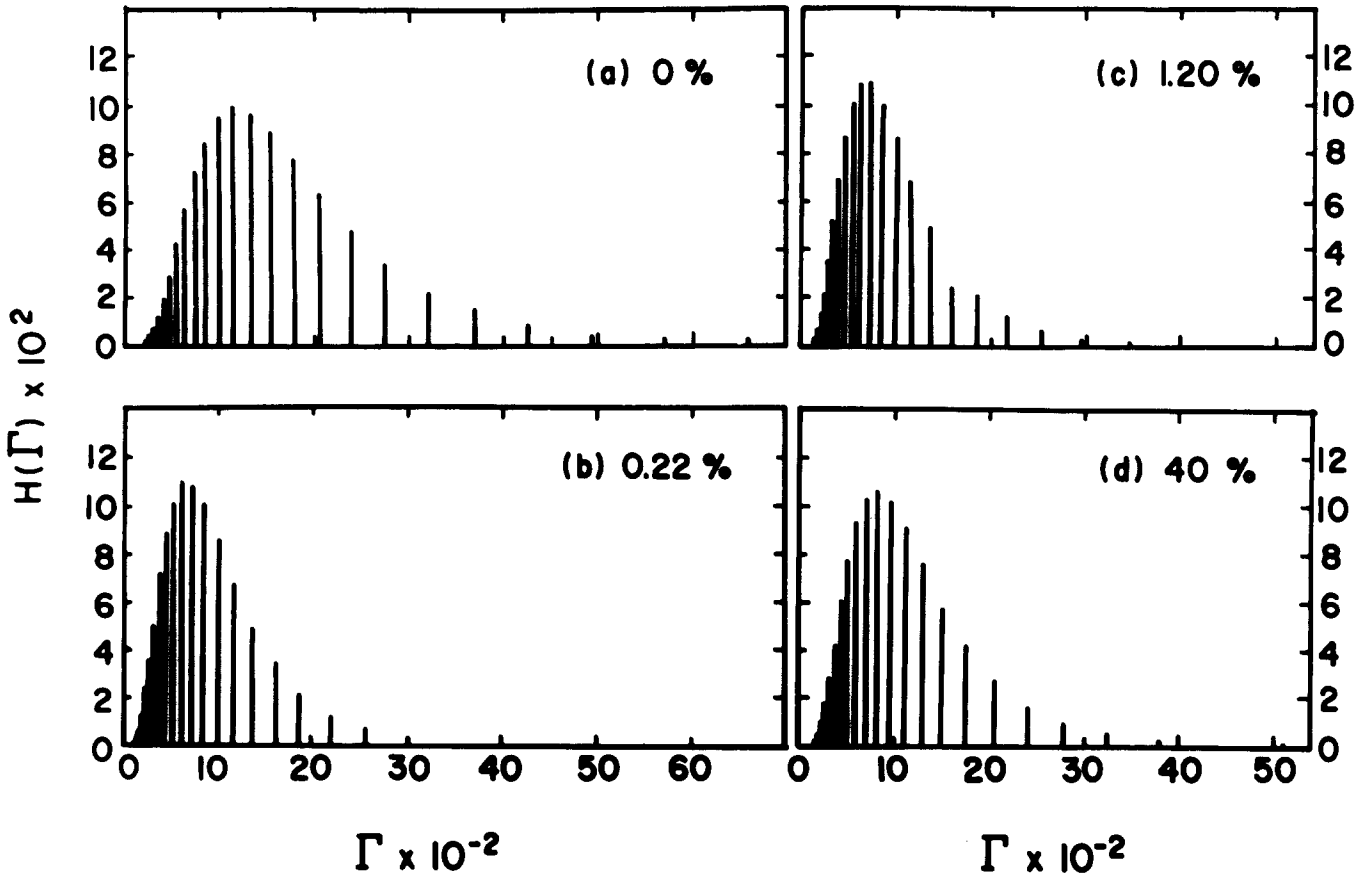

Figure 10 Histogram $H(\Gamma_j)$ obtained in the unimodal analysis of the autocorrelation function $A(\tau)$ plotted against delay time τ shown in *Figure 9*. The measurements were done for water solution of HPC with various contents of glyoxal: (a) 0%, (b) 0.22%, (c) 1.20% and (d) 40%

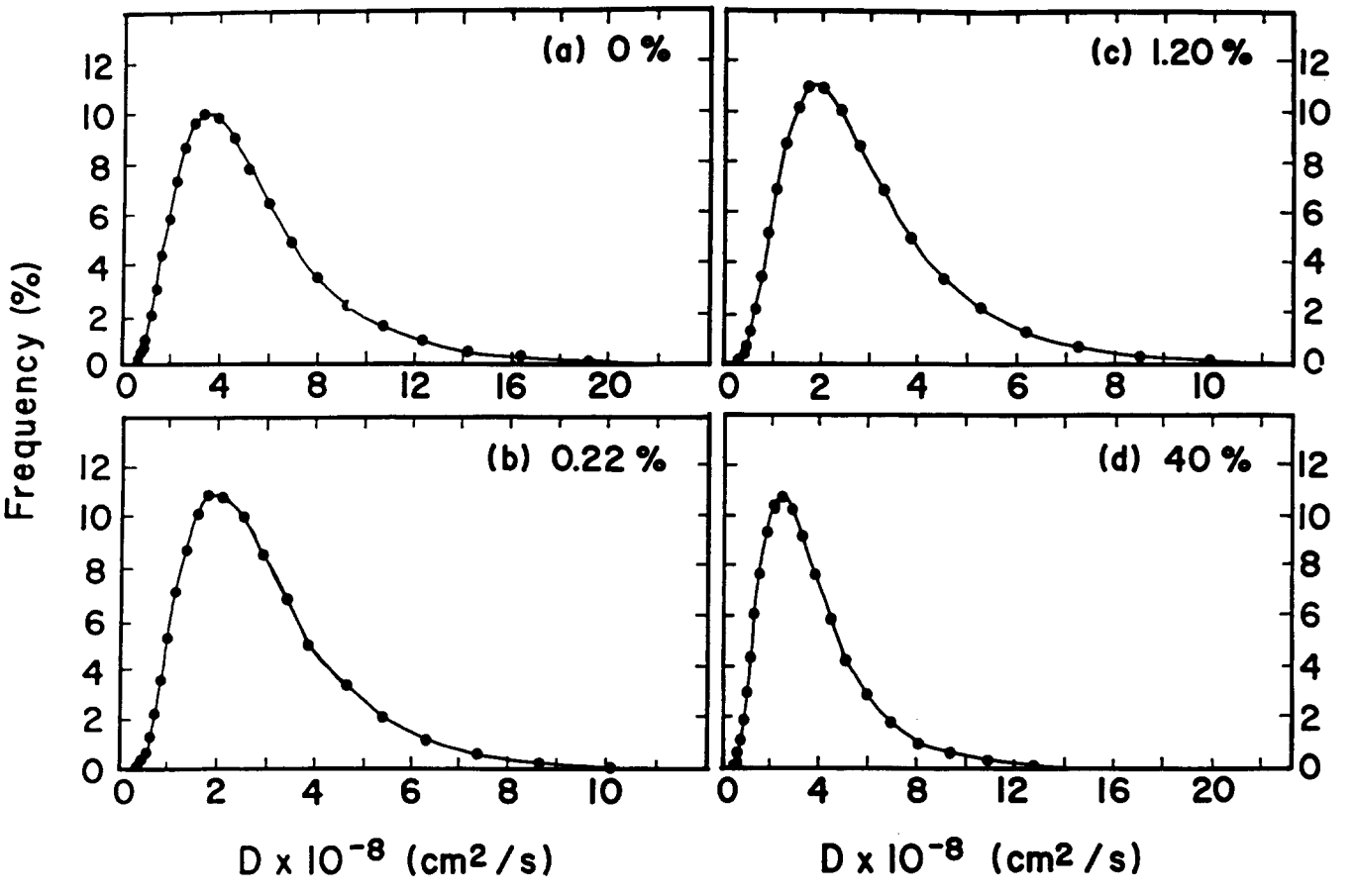

Figure 11 Distribution function of diffusion coefficient of HPC molecules in water solutions with various contents of glyoxal: (a) 0%, (b) 0.22%, (c) 1.20% and (d) 40%

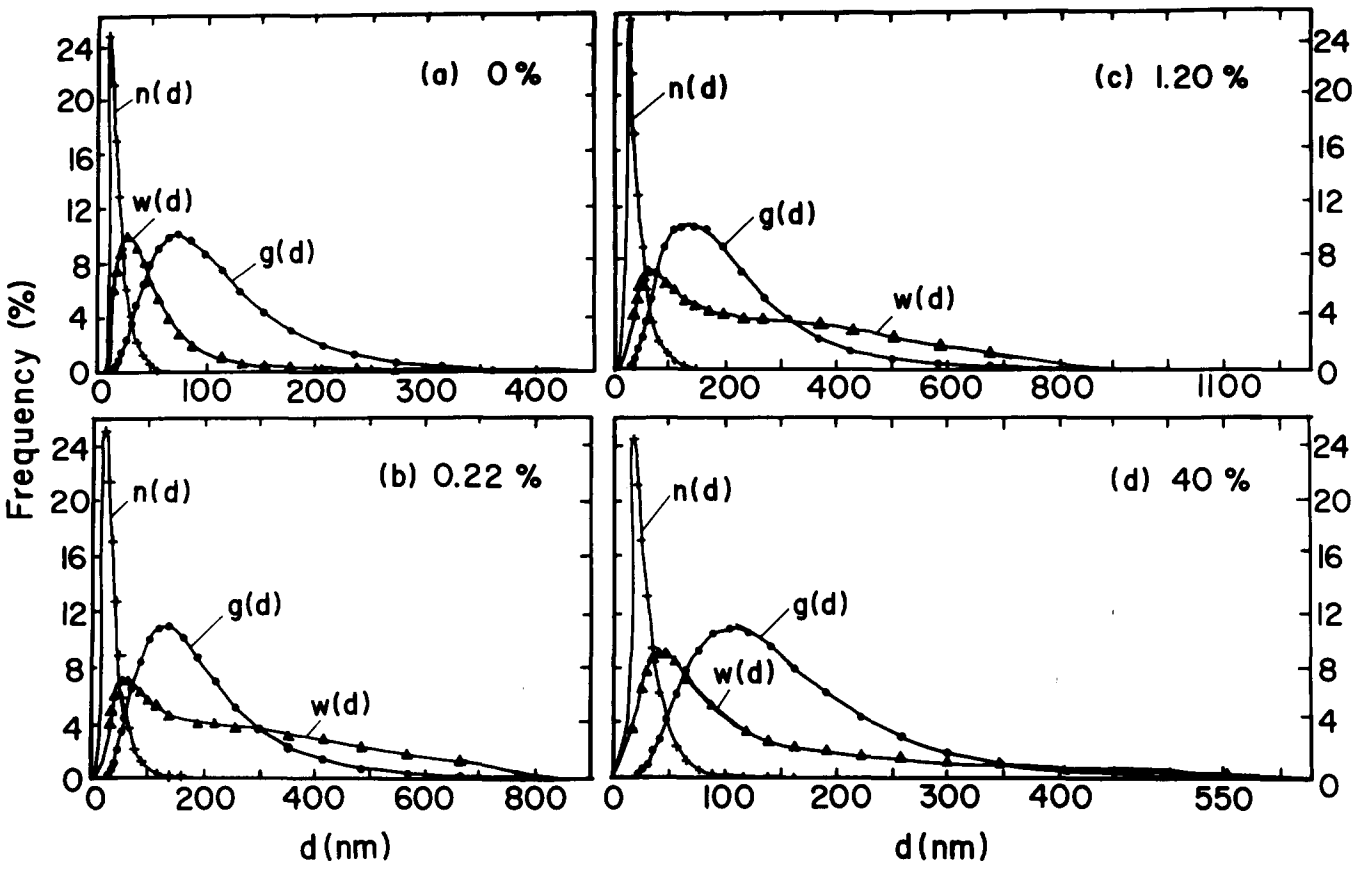

Figure 12 Distributions of fractions $g(d)$, $w(d)$ and $n(d)$ with particle size in water solutions with various contents of glyoxal: (a) 0%, (b) 0.22%, (c) 1.20% and (d) 40%

Table 2 Diffusion coefficient and Stokes radius of HPC molecules in water and ethanol solutions with different glyoxal contents

Solvent	Glyoxal (wt%)	Diffusion coefficient (10^{-8} cm^2 s^{-1})	Stokes radius (nm)
Water	0	2.83	87.0
	0.22	2.25	110.5
	1.20	2.24	111.5
	40	2.49	99.5
Ethanol	0	4.43	35.5
	0.22	4.40	35.7
	1.20	3.61	43.6
	40	2.37	66.3

This indicates that the chain mobility increases with main-chain scission. Interestingly, the change in the diffusion coefficient with increasing glyoxal content is in good agreement with the changes of morphology and mechanical properties of the resultant cast films as shown in *Figures 2–8*.

Figure 12 shows the distributions of $g(d)$, $w(d)$ and $n(d)$. The three distributions indicate that the Stokes radius corresponding to the degree of aggregation of HPC chains becomes larger with increasing glyoxal content up to 1.2%. However, the radius decreases at glyoxal contents $\geqslant$1.2%. Therefore, the representation in *Figure 12* is thought to be one of the most suitable methods to represent the change in the particle size with the content of glyoxal.

On the other hand, the diffusion coefficient can also be calculated from the mean delay rate by using a cumulant method. The relationship between the cumulant and the moment expressions for $g^{(1)}(\tau)$ may be represented as:

$$\ln|g^{(1)}(\tau)| = \sum_{n=1}^{\infty} K_n(\Gamma)[(-\tau)^n/n!]$$

$$= -\bar{\Gamma}\tau + \frac{1}{2!}\mu_2\tau^2 - \frac{1}{3!}\mu_3\tau^3$$

$$+ \frac{1}{4!}(\mu_4 - 3\mu_2^2)\tau^4 + \cdots \qquad (15)$$

where K_n is the nth cumulant, and μ_n is the nth moment about the mean of $G(\Gamma)$ as follows:

$$\mu_n = \int_0^{\infty} (\Gamma - \bar{\Gamma})^n G(\Gamma)\,d\Gamma \qquad (16)$$

Thus, the average diffusion coefficient $\langle D \rangle$ may be given by:

$$\langle D \rangle = \bar{\Gamma}/q^2 \qquad (K_1 = \mu_1 = \bar{\Gamma}) \qquad (17)$$

Thus, the Stokes radius may be given as:

$$d = kT/6\pi\eta\langle D \rangle \qquad (18)$$

where T is the absolute temperature, k is the Boltzmann constant and η is the solvent viscosity.

Table 2 summarizes diffusion coefficient $\langle D \rangle$ and the Stokes radius d, estimated by the cumulative method. The Stokes radius in the HPC–water system is larger than that in HPC–ethanol, indicating that water is a good solvent for HPC in comparison with ethanol. The particle size becomes bigger as the crosslinking effect is more pronounced by introducing glyoxal up to 1.20%.

This indicates that intermolecular chain crosslinking causes a significant effect on the increase in the Stokes radius by aggregation of several chains. In the case of water solution containing 40% glyoxal, however, the particle size becomes smaller than that in water solution containing 1.20% glyoxal. This is probably due to main-chain scission during the crosslinking process owing to violent chemical reaction. By contrast, the Stokes radius increases with glyoxal content in the HPC–water system. This indicates that, since main-chain scission is not so drastic even at 40% glyoxal content, the crosslinking reaction in the HPC–ethanol system is not active in comparison with that in HPC–water. Actually, the resultant film cast from water solution in *Figure 7* shows effective heat resistance beyond 300°C in the case of 6.25% glyoxal but cannot be maintained at 150°C in the case of 40% glyoxal. In contrast, the heat-resistance effect of the resultant film cast from ethanol is independent of the content of glyoxal and can be maintained at 250°C higher than the breaking point of uncrosslinked HPC film (180°C).

CONCLUSIONS

The crosslinking of HPC molecules was performed in water and ethanol solutions containing glyoxal. The degree of crosslinking was dependent upon the content of glyoxal. This tendency is more significant in the HPC–water system. When an excess of glyoxal was introduced in the HPC–water system, drastic main-chain scission occurred. The scission causes drastic decreases in the Young's modulus and tensile strength. In particular, when 40% glyoxal was introduced, the Hv light scattering from the resultant film displayed a circular pattern, indicating scattering from a random array of crystallites that are small compared with the wavelength of the incident laser beam. The corresponding optical micrographs show a dark field of vision. Furthermore, the diffraction intensity from the (1 0 0) plane of the corresponding film was the weakest among those of all the crosslinked films. Thus it turned out that excess glyoxal hampers the heat-resistance effect and the improvement of mechanical properties. The main-chain scission was confirmed by the Stokes radius distribution of HPC chains in water and ethanol solutions using dynamic light scattering. The radius became larger with increasing glyoxal content, but at 40% glyoxal the size became smaller. At present, it is very difficult to discuss the crosslinking mechanism quantitatively by the dynamic light scattering technique, since the HPC molecules used in this experiment are polydisperse with wide molecular-weight distribution. Further consideration must be given to obtaining a more quantitative answer using HPC molecules with a narrow distribution by the method of Wirick *et al.*[2].

ACKNOWLEDGEMENTS

We thank Dr Tsunashima, Chemical Institute of Kyoto University, Uji, Japan, for valuable comments and suggestions for measuring autocorrelation functions. We are also indebted to Professor Taga, Faculty of Engineering, Yamagata University, Yonezawa, Japan, for valuable discussions and suggestions for the preparation of crosslinked HPC films and Dr Sudo, also of Yamagata University, for measuring molar substitution (MS), $\bar{M}_w$ and $\bar{M}_n$.

REFERENCES

1 Samuels, R. J. *J. Polym. Sci. (A-2)* 1969, **7**, 1197
2 Wirick, M. G. and Waldman, M. H. *J. Appl. Polym. Sci.* 1970, **14**, 579
3 Sawatari, C., Shimogiri, S. and Matsuo, M. *Macromolecules* 1987, **20**, 1033
4 Sawatari, C. and Matsuo, M. *Polymer* 1989, **30**, 1603
5 Matsuo, M., Sawatari, C. and Ohhata, T. *Macromolecules* 1988, **21**, 1317
6 Sawatari, C., Satoh, S. and Matsuo, M. *Polymer* 1990, **31**, 1456
7 Berne, B. J. and Pecora, R. 'Dynamic Light Scattering', Wiley, New York, 1976
8 Chu, B. 'Laser Light Scattering', Academic Press, New York, 1974
9 Koppel, D. E. *J. Chem. Phys.* 1972, **57**, 4814
10 Gulari, E., Gulari, E., Tsunashima, Y. and Chu, B. *J. Chem. Phys.* 1979, **70**, 3965
11 Gulari, E., Gulari, E., Tsunashima, Y. and Chu, B. *Polymer* 1979, **20**, 347
12 Tsunashima, Y., Nemoto, N. and Kurata, M. *Macromolecules* 1983, **16**, 584
13 Hirata, M. and Tsunashima, Y. *Macromolecules* 1989, **22**, 249
14 Rhodes, M. B. and Stein, R. S. *J. Polym. Sci. (A-2)* 1969, **7**, 1539
15 Matsuo, M., Nomura, S., Hashimoto, T. and Kawai, H. *Polym. J.* 1974, **6**, 151
16 Iida, M., Sawatari, C. and Matsuo, M. *J. Chem. Soc., Faraday Trans. (II)* 1984, **80**, 1599